

UCSF

UC San Francisco Previously Published Works

Title

4-1BB Delineates Distinct Activation Status of Exhausted Tumor-Infiltrating CD8+ T Cells in Hepatocellular Carcinoma

Permalink

<https://escholarship.org/uc/item/0n01x88j>

Journal

Hepatology, 71(3)

ISSN

0270-9139

Authors

Kim, Hyung-Don
Park, Seongyeol
Jeong, Seongju
[et al.](#)

Publication Date


2020-03-01

DOI

10.1002/hep.30881

Peer reviewed

4-1BB Delineates Distinct Activation Status of Exhausted Tumor-Infiltrating CD8⁺ T Cells in Hepatocellular Carcinoma

Hyung-Don Kim,¹ Seongyeol Park,¹ Seongju Jeong,² Yong Joon Lee,¹ Hoyoung Lee,² Chang Gon Kim,¹ Kyung Hwan Kim,¹ Seung-Mo Hong,³ Jung-Yun Lee,⁴ Sunghoon Kim,⁴ Hong Kwan Kim,⁵ Byung Soh Min,⁶ Jong Hee Chang,⁷ Young Seok Ju,^{1,2} Eui-Cheol Shin,^{1,2} Gi-Won Song,⁸ Shin Hwang,⁸ and Su-Hyung Park ^{1,2}

BACKGROUND AND AIMS: Targeting costimulatory receptors with agonistic antibodies is a promising cancer immunotherapy option. We aimed to investigate costimulatory receptor expression, particularly 4-1BB (CD137 or tumor necrosis factor receptor superfamily member 9), on tumor-infiltrating CD8⁺ T cells (CD8⁺ tumor-infiltrating lymphocytes [TILs]) and its association with distinct T-cell activation features among exhausted CD8⁺ TILs in hepatocellular carcinoma (HCC).

APPROACH AND RESULTS: Tumor tissues, adjacent non-tumor tissues, and peripheral blood were collected from HCC patients undergoing surgical resection (n = 79). Lymphocytes were isolated and used for multicolor flow cytometry, RNA-sequencing, and *in vitro* functional restoration assays. Among the examined costimulatory receptors, 4-1BB was most prominently expressed on CD8⁺ TILs. 4-1BB expression was almost exclusively detected on CD8⁺ T cells in the tumor—especially on programmed death 1 (PD-1)^{high} cells and not PD-1^{int} and PD-1^{neg} cells. Compared to PD-1^{int} and 4-1BB^{neg}PD-1^{high} CD8⁺ TILs, 4-1BB^{pos}PD-1^{high} CD8⁺ TILs exhibited higher levels of tumor reactivity and T-cell activation markers and significant enrichment for T-cell activation gene signatures. Per-patient analysis revealed positive correlations between

percentages of 4-1BB^{pos} cells among CD8⁺ TILs and levels of parameters of tumor reactivity and T-cell activation. Among highly exhausted PD-1^{high} CD8⁺ TILs, 4-1BB^{pos} cells harbored higher proportions of cells with proliferative and reinvigoration potential. Our 4-1BB-related gene signature predicted survival outcomes of HCC patients in the The Cancer Genome Atlas cohort. 4-1BB agonistic antibodies enhanced the function of CD8⁺ TILs and further enhanced the anti-PD-1-mediated reinvigoration of CD8⁺ TILs, especially in cases showing high levels of T-cell activation.

CONCLUSION: 4-1BB expression on CD8⁺ TILs represents a distinct activation state among highly exhausted CD8⁺ T cells in HCC. 4-1BB costimulation with agonistic antibodies may be a promising strategy for treating HCCs exhibiting prominent T-cell activation. (HEPATOLOGY 2020;71:955-971).

Immune checkpoint inhibitors (ICIs) have revolutionized the treatment of various cancer types, and several agents targeting the programmed death 1 (PD-1)/programmed death-ligand 1 and cytotoxic T-lymphocyte-associated protein 4 pathways are currently available for clinical use.⁽¹⁾ Recent clinical trials

Abbreviations: CD8⁺ TILs, tumor-infiltrating CD8⁺ T cells; CTV, CellTrace Violet; DEGs, differentially expressed genes; DR3, death receptor 3; FACS, fluorescence-activated cell sorting; GITR, glucocorticoid-induced tumor necrosis factor receptor-related protein; GSEA, gene set enrichment analysis; GSVA, gene set variation analysis; HCC, hepatocellular carcinoma; ICI, immune checkpoint inhibitor; IFN- γ , interferon-gamma; IHL, intrahepatic lymphocyte; HLA, human leukocyte antigen; HVEM, herpesvirus entry mediator; PBMC, peripheral blood mononuclear cell; PD-1, programmed cell death protein 1; RNA-seq, RNA-sequencing; SI, stimulation index; TCF-1, T-cell factor 1; TCGA, The Cancer Genome Atlas; TCR, T-cell receptor; TIL, tumor-infiltrating lymphocyte; TME, tumor microenvironment; TNF- α , tumor necrosis factor alpha; TNFR2, tumor necrosis factor receptor 2; TNFRSF, tumor necrosis factor receptor superfamily member.

Received March 12, 2019; accepted July 19, 2019.

Additional Supporting Information may be found at onlinelibrary.wiley.com/doi/10.1002/hep.30881/supinfo.

Supported by the National Research Foundation of Korea (NRF) grant funded by the Korea government (MSIT; NRF-2019R1A2C2005176; to S.H.P.) and by a grant from the Korea Health Technology R&D Project through the Korea Health Industry Development Institute (KHIDI), funded by the Ministry of Health & Welfare, Republic of Korea (HI15C2859; to S.H.P.). This work was also supported by the KAIST Future Systems Healthcare Project from the Ministry of Science and ICT (to S.H.P.), Young Medical Scientist Research Grant through the Deawoong Foundation (DF-201906-0000003; to H.D.K.), and the Global Ph.D. Fellowship from the National Research Foundation of Korea (NRF-2016H1A2A1906766; to H.D.K.).

of anti-PD-1 therapy in patients with advanced hepatocellular carcinoma (HCC) show objective response rates of 16%–20%,^(2,3) prompting U.S. Food and Drug Administration approval of the anti-PD-1 monoclonal antibodies, nivolumab and pembrolizumab, for use in HCC. However, the majority of HCC patients receiving anti-PD-1 therapy still do not derive clinical benefit, highlighting the urgent need for immunotherapeutic strategies with improved therapeutic efficacy. To this end, research groups are investigating the use of various ICI-based therapeutic strategies in combination with targeted agents, locoregional therapy, and other forms of immunotherapy.⁽⁴⁾

One promising therapeutic approach involves targeting costimulatory receptors, such as 4-1BB, glucocorticoid-induced tumor necrosis factor receptor-related protein (GITR), and OX-40, with agonistic antibodies.^(1,5-7) In addition to T-cell receptor (TCR) signaling, costimulatory signaling is critical for full T-cell activation and positively regulates T-cell differentiation, effector function, survival, and memory formation.^(8,9) Agonistic antibodies to costimulatory receptors may be used to potentiate these

functional responses against tumors.^(1,5-7) Among costimulatory receptors, 4-1BB (tumor necrosis factor receptor superfamily member [TNFRSF] 9 or CD137) is considered one of the most compelling targets because of its capacity to activate exhausted T cells^(5,10-12) and its potent antitumor efficacy shown in preclinical models.^(5,11,13,14) Several clinical trials are evaluating the efficacy of 4-1BB agonists combined with other immunotherapeutic strategies in multiple cancer types.⁽⁵⁾ However, little is known about the expression patterns of costimulatory receptors such as 4-1BB on tumor-infiltrating T cells or about the immunological and clinical implications of costimulatory receptor expression in HCC patients. Given the vital role of CD8⁺ T cells in eliciting antitumor functional responses⁽¹⁵⁻¹⁷⁾ and their substantial heterogeneity among HCCs,⁽¹⁸⁻²⁰⁾ the rational development of therapies targeting costimulatory receptors will require investigation of the expression patterns of costimulatory receptors on tumor-infiltrating CD8⁺ T cells (CD8⁺ tumor-infiltrating lymphocytes [TILs]).

Many costimulatory receptors exhibit activation-induced expression on T cells,^(8,9) suggesting

© 2019 The Authors. HEPATOLOGY published by Wiley Periodicals, Inc., on behalf of American Association for the Study of Liver Diseases. This is an open access article under the terms of the Creative Commons Attribution-NonCommercial License, which permits use, distribution and reproduction in any medium, provided the original work is properly cited and is not used for commercial purposes.

View this article online at wileyonlinelibrary.com.

DOI 10.1002/hep.30881

Potential conflict of interest: Nothing to report.

ARTICLE INFORMATION:

From the ¹Graduate School of Medical Science and Engineering, Korea Advanced Institute of Science and Technology, Daejeon, Republic of Korea; ²Biomedical Science and Engineering Interdisciplinary Program, Korea Advanced Institute of Science and Technology, Daejeon, Republic of Korea; ³Department of Pathology, Asan Medical Center, University of Ulsan College of Medicine, Seoul, Republic of Korea; ⁴Department of Obstetrics and Gynecology, Severance Hospital, Yonsei University College of Medicine, Seoul, Republic of Korea; ⁵Department of Thoracic and Cardiovascular Surgery, Samsung Medical Center, Sungkyunkwan University School of Medicine, Seoul, Republic of Korea; ⁶Department of Surgery, Severance Hospital, Yonsei University College of Medicine, Seoul, Republic of Korea; ⁷Department of Neurosurgery, Severance Hospital, Yonsei University College of Medicine, Seoul, Republic of Korea; ⁸Department of Surgery, Asan Medical Center, University of Ulsan College of Medicine, Seoul, Republic of Korea.

ADDRESS CORRESPONDENCE AND REPRINT REQUESTS TO:

Su-Hyung Park, Ph.D.
Laboratory of Translational Immunology and Vaccinology
Graduate School of Medical Science and Engineering
Korea Advanced Institute of Science and Technology
291 Daehak-ro
Daejeon 34141, Republic of Korea
E-mail: park3@kaist.ac.kr
Tel.: +82-42-350-4248;
or

Shin Hwang, M.D., Ph.D.
Division of Hepatobiliary Surgery and Liver Transplantation
Department of Surgery, Asan Medical Center
University of Ulsan College of Medicine
Seoul, Republic of Korea
88, Olympic-ro 43-gil
Songpa-gu
Seoul, 05505, Korea
E-mail: shwang@amc.seoul.kr
Tel.: +82-2-3010-3930

that their expression levels may represent the degree of T-cell activation, and therapeutic costimulation conceptually targets T cells that have already been activated in the tumor microenvironment (TME). Therefore, delineation of the T-cell activation features associated with costimulatory receptor expression will provide insights regarding how to maximize anti-HCC T-cell activation to improve the therapeutic efficacy of ICIs, as well as help identify additional targets involved in T-cell activation in the TME. In particular, identification of a distinct T-cell activation state among heterogeneously exhausted T cells could guide the development of T-cell-activating approaches specifically targeting CD8⁺ TIL populations that have rigorously engaged in antitumor responses and subsequently acquired exhausted phenotypes. However, the heterogeneity of exhausted CD8⁺ TILs in the context of T-cell activation in HCC remains largely unknown.

In this study, we aimed to comprehensively investigate the expression of costimulatory receptors on CD8⁺ TILs and its association with distinct features of T-cell activation among exhausted CD8⁺ TILs in HCC. We focused on costimulatory receptor 4-1BB because of its prominent expression on CD8⁺ TILs in HCC patients. We further examined the impact of 4-1BB costimulation with agonistic antibodies on the functional responses of exhausted CD8⁺ TILs. Our results show that 4-1BB expression identifies a distinctly activated population of exhausted CD8⁺ TILs and suggest that 4-1BB costimulation may be a promising strategy for HCC patients with prominent T-cell activation.

Materials and Methods

STUDY PATIENTS AND CLINICAL SAMPLES

Clinical samples were obtained from a prospective cohort of 79 patients with pathologically confirmed HCC who underwent surgical resection at Asan Medical Center (Seoul, Korea) between April 2016 and April 2019. Fresh tumor tissue, adjacent nontumor liver tissue, and whole-blood samples were collected. Table 1 summarizes the clinical characteristics of the study patients. We also obtained fresh tumor tissues from patients with other cancer types, and the

TABLE 1. Clinical Characteristics of the Study Patients With HCC

Variable	n = 79
Age (years)	60.1 ± 9.9
Male sex	61 (77.9%)
Etiology	
HBV	58 (73.4%)
HCV	6 (7.6%)
NBNC	15 (18.9%)
ALT (IU/mL)	26 (18-50)
INR	1.06 ± 0.09
Total bilirubin (mg/dL)	0.6 ± 0.3
Albumin (g/dL)	3.8 ± 0.4
AFP (ng/mL)	9.8 (3.6-231.0)
Liver cirrhosis	26 (32.9%)
Microvascular invasion	37 (46.8%)
Tumor diameter (cm)	4.3 (3.1-6.7)
Edmondson-Steiner grade 3/4 (worst grade)	58 (74.7%)

Data are presented as no. (%) or mean ± SD or median (interquartile range).

Abbreviations: HBV, hepatitis B virus; HCV, hepatitis C virus; NBNC, non-B non-C; ALT, alanine aminotransferase; INR, international normalized ratio; AFP, alpha-fetoprotein.

corresponding data are summarized in Supporting Table S1. All included patients provided written informed consent, and this study was approved by the institutional review board.

Peripheral blood mononuclear cells (PBMCs) were isolated from whole blood by standard Ficoll-Paque (GE Healthcare, Uppsala, Sweden) density gradient centrifugation. Intrahepatic lymphocytes (IHLs) and TILs were isolated from tissue samples as described.⁽¹⁸⁾ Briefly, tissue samples were cut into small pieces (2-4 mm) and then transferred to a gentle MACS C-Tube containing a mixture of enzymes (Milteny Biotec, Bergisch Gladbach, Germany). Next, samples were mechanically homogenized and enzymatically digested using the gentle MACS Octo Dissociator (Milteny Biotec). The resulting cell suspension was passed through a 70- μ m cell strainer, and then the cells were washed and cryopreserved.

FLOW CYTOMETRY AND IMMUNOPHENOTYPING

Cells were stained using the LIVE/DEAD fixable red dead cell stain kit (Invitrogen, Carlsbad, CA) to gate out dead cells. Cells were washed once and

then stained with fluorochrome-conjugated antibodies against surface markers for 30 minutes at 4°C, followed by a second wash. For intracellular staining, cells were then fixed and permeabilized using a fork-head box protein P3 staining buffer kit (eBioscience, San Diego, CA) and then stained for intracellular proteins. Flow cytometry was performed using an LSR II instrument and FACSDiva software (BD Biosciences, San Jose, CA). Data were analyzed using FlowJo software (Treestar, San Carlos, CA).

RNA-SEQUENCING AND DATA ANALYSIS

RNA-sequencing (RNA-seq) was performed on PD-1^{int}, 4-1BB^{neg}PD-1^{high}, and 4-1BB^{pos}PD-1^{high} CD8⁺ TILs (n = 5) that were sorted using a FACS Aria II cell sorter (BD Biosciences), as well as on total CD8⁺ TILs sorted using CD8 Microbeads (n = 10; Miltenyi Biotec). Each sorted cells sample had a purity of >90%. Sorted cells were cryopreserved in TRIzol reagent (Invitrogen), and RNA extraction was performed following the manufacturer's instructions.

Total RNA quality was assessed using the Agilent 2100 Bioanalyzer System. Extracted RNA samples were processed using the QuantSeq 3' mRNA-Seq Library Prep Kit (Lexogen, Vienna, Austria) and sequenced on an Illumina NextSeq 500. Read counts were normalized for effective library size, and differentially expressed genes (DEGs) were analyzed using DESeq2.⁽²¹⁾ DEGs were defined by a *P* value of <0.05 and an absolute fold change of >2. Based on *P* values, we determined the top 50 genes that were significantly up- or down-regulated between 4-1BB^{neg}PD-1^{high} and 4-1BB^{pos}PD-1^{high} CD8⁺ TILs. Gene set enrichment analysis (GSEA) was utilized to assess the enrichment of specific gene sets.⁽²²⁾ For the RNA-seq data, the Gene Expression Omnibus accession numbers are GSE132810 (for PD-1^{int}, 4-1BB^{neg}PD-1^{high}, and 4-1BB^{pos}PD-1^{high} CD8⁺ TILs) and GSE132812 (for total CD8⁺ TILs).

T-CELL ACTIVATION GENE SIGNATURES FROM THE LITERATURE

The "Activation-specific module" was directly obtained from the "ACT module" identified by Singer et al.⁽²³⁾ The "CD8 *in vivo* activation" gene set was

defined as the intersection of the DEGs between effector and naïve CD8⁺ T cells and of the DEGs between effector and memory CD8⁺ T cells in the article by Sankar et al.⁽²⁴⁾ The "Effector and exhausted gene" set was defined as the sum of "cluster 2" and "cluster 6" as identified by Wherry et al.,⁽²⁵⁾ which represents the genes commonly up-regulated in effector and exhausted T cells. The "Acutely stimulated CD8⁺ T cell" gene set comprised DEGs that were up-regulated in activated T cells compared to naïve T cells in the study by Giordano et al.⁽²⁶⁾

THE CANCER GENOME ATLAS DATA ANALYSIS

RNA-seq data from the 370 HCC patients in The Cancer Genome Atlas (TCGA) were obtained from the GDC Data Portal (National Cancer Institute, Rockville, MD). Gene set variation analysis (GSVA) was performed using the R package, GSVA. Then, the enrichment score for the gene signatures was calculated by GSVA.⁽²⁷⁾ Gene expression and survival data of an independent HCC cohort were obtained from GSE 76427⁽²⁸⁾ and analyzed in the same manner. To conceptually compare the survival outcomes of the subcohorts, we used the enrichment score cutoff determined by the maximal chi-square method using the R package, Maxstat, for each cohort.⁽²⁹⁾

IN VITRO FUNCTIONAL ASSAY

To represent costimulation under *in vivo* conditions, TILs were incubated at 37°C for 30 minutes with 10 µg/mL of agonistic antibodies for 4-1BB (provided by ABL Bio, Seongnam, South Korea), GITR (79053-2; BPS Bioscience, San Diego, CA), tumor necrosis factor receptor 2 (TNFR2; HM2007; Hycult Biotech, Uden, The Netherlands), or CD30 (81337; R&D Systems, Minneapolis, MN) or with the isotype controls, QA16A15 (Bio-Legend), QA16A12 (Bio-Legend), MOPC-21 (Bio-Legend), or 20116 (R&D Systems). Cells were then transferred to wells containing soluble anti-CD3 antibody (1 ng/mL; OKT-3; eBioscience) and either 10 µg/mL of blocking antibodies for PD-1 (EH12.2H7; Bio-Legend) or isotype control (MOPC-21; Bio-Legend). To measure CD8⁺ TIL proliferation, cells were labeled with CellTrace Violet (CTV; Invitrogen) and cultured for 72 hours. The mitotic index was calculated according

to mitotic events, using the absolute number of precursor cells and the number of cells in each mitotic division. To standardize the baseline difference in proliferative capacity, we determined the stimulation index (SI) by dividing the mitotic index of the samples treated with anti-PD-1 and/or anti-4-1BB by that of the isotype control-treated samples. We assessed interferon-gamma (IFN- γ) and tumor necrosis factor alpha (TNF- α) production after 36 hours of culture. Brefeldin A and monensin (BD Biosciences) were added for the last 12 hours of incubation.

Results

4-1BB IS PROMINENTLY EXPRESSED ON CD8⁺ TILs, ESPECIALLY ON PD-1^{high} CELLS

We first examined the expression levels of various activation-induced costimulatory receptors of the TNFRSF⁽⁹⁾ on CD8⁺ TILs from HCC patients. Among the examined costimulatory receptors, 4-1BB was more prominently expressed on CD8⁺ TILs compared to GITR, TNFR2, death receptor 3 (DR3), OX-40, herpesvirus entry mediator (HVEM), and CD30 (Fig. 1A). To further delineate HCC-specific aspects of costimulatory receptor expression, we also analyzed costimulatory receptor expression on CD8⁺ TILs from other cancer types (Supporting Table S1). Multicancer analysis of 4-1BB expression revealed that the percentage of 4-1BB^{pos} CD8⁺ TILs was higher in HCC than in the other examined cancer types, although the difference between HCC and ovarian cancer was not statistically significant (Fig. 1B). In contrast, the percentages of CD8⁺ TILs expressing other costimulatory receptors were not higher, or were even lower, in HCC compared to in other cancer types (Supporting Fig. S1). Furthermore, among the examined TNFRSF costimulatory receptors, 4-1BB was not the one most highly expressed in other examined cancer types (Supporting Fig. S2). These data indicate that prominent 4-1BB expression on CD8⁺ TILs may be a notable feature of HCC; thus, we focused on 4-1BB expression in our further investigations of the activation-related features of CD8⁺ TILs and of its potential as an immunotherapeutic target for HCC patients.

Next, we examined 4-1BB expression across different cellular fractions (i.e., PBMCs, IHLs, and TILs) and immunophenotypes of tumor-antigen-specific CD8⁺ T cells using a human leukocyte antigen (HLA)-A*0201 dextramer specific to NY-ESO-1₁₅₇₋₁₆₅. Total CD8⁺ T cells as well as NY-ESO-1₁₅₇₋₁₆₅-specific CD8⁺ T cells in the TIL fraction included significantly higher percentages of 4-1BB^{pos} cells compared to the IHL and PBMC fractions (Fig. 1C). The percentage of 4-1BB^{pos} cells among CD8⁺ TILs did not differ among HCCs with different etiologies (Supporting Fig. S3).

We recently demonstrated that PD-1⁺ CD8⁺ TILs from HCC patients can be subdivided into PD-1^{int} and PD-1^{high} CD8⁺ TILs and that the latter group shows features of more-severe T-cell exhaustion.⁽¹⁸⁾ Another recent study found that PD-1^{high} CD8⁺ TILs exhibit high tumor reactivity.⁽³⁰⁾ Therefore, we next examined 4-1BB expression on CD8⁺ TILs according to differential PD-1 expression, to investigate the role of 4-1BB in the context of T-cell exhaustion and tumor reactivity. Interestingly, 4-1BB was almost exclusively expressed on PD-1^{high} CD8⁺ TILs (Fig. 1D). Most PD-1^{int} and PD-1^{neg} CD8⁺ TILs showed no 4-1BB expression (Fig. 1D). A similar pattern was observed for NY-ESO-1₁₅₇-specific CD8⁺ TILs (Fig. 1C, right panel). Frequencies of 4-1BB^{pos} cells among total and NY-ESO-1₁₅₇-specific CD8⁺ TILs were positively correlated with frequencies of PD-1^{high} total and NY-ESO-1₁₅₇-specific CD8⁺ TILs (Fig. 1E).

4-1BB-EXPRESSING PD-1^{high} CD8⁺ TILs FEATURE IMMUNOPHENOTYPICALLY AND TRANSCRIPTIONALLY PROMINENT T-CELL ACTIVATION

Exhausted CD8⁺ T cells are considered a primary target for therapeutic interventions involving ICIs.^(15-17,30) Therefore, the delineation of distinct features of exhausted CD8⁺ TILs based on T-cell activation status could help direct therapeutic strategies to maximize CD8⁺ TIL activation and assess the degree of preexisting T-cell activation that can be targeted by immunotherapy. To further examine the immunological role of 4-1BB as a T-cell-activating receptor in phenotypically exhausted CD8⁺ TILs,

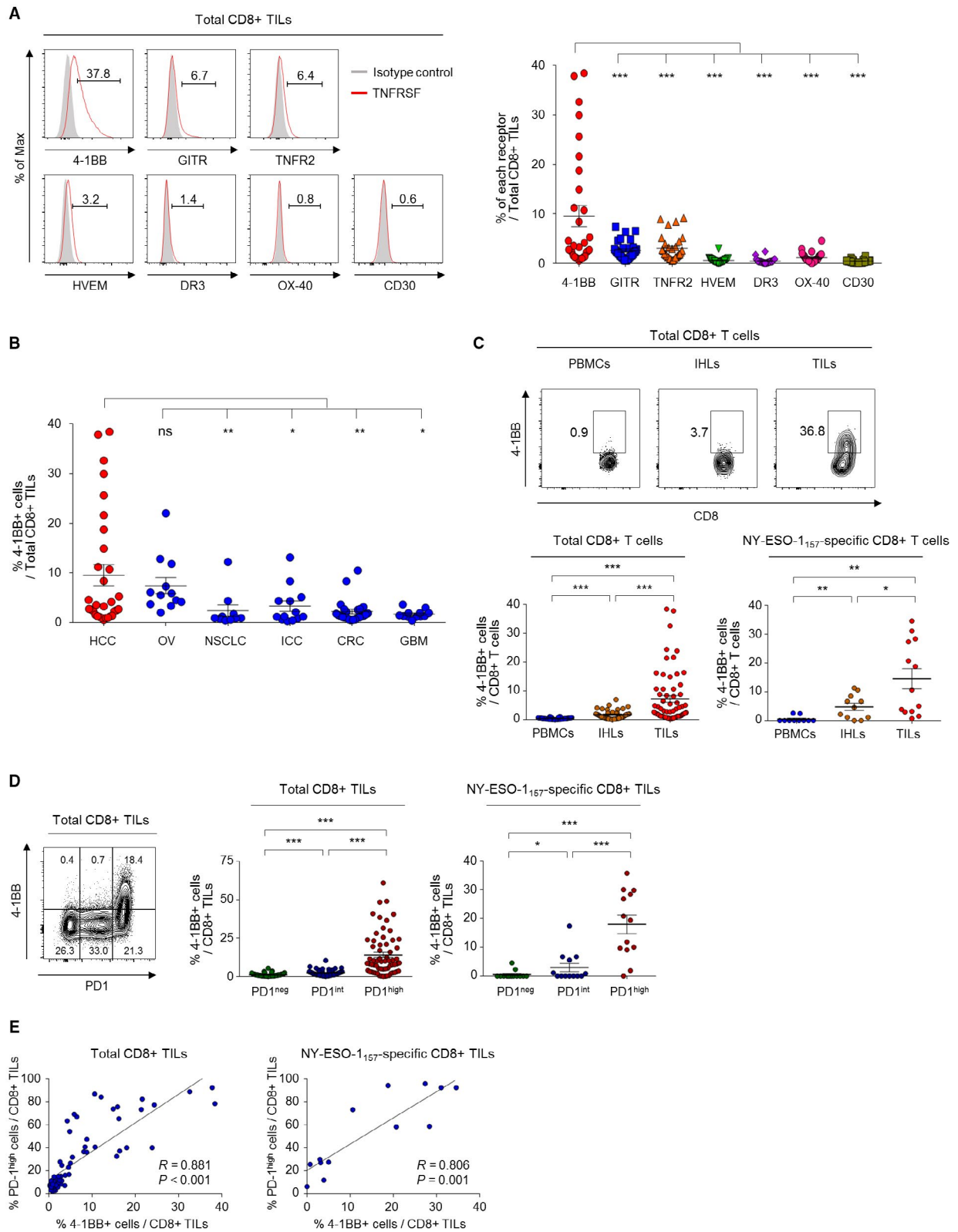


FIG. 1. Compared to other costimulatory receptors, 4-1BB is more prominently expressed on CD8⁺ TILs, especially on PD-1^{high} cells. (A) The percentage of CD8⁺ TILs that expressed various activation-induced costimulatory receptors belonging to the TNFRSF. Left panel shows representative flow cytometry histograms. (B) Percentages of 4-1BB^{pos} CD8⁺ TILs in various cancer types: OV, ovarian cancer; NSCLC, non-small-cell lung cancer; ICC, intrahepatic cholangiocellular carcinoma; CRC, colorectal cancer; and GBM, glioblastoma multiforme. (C) 4-1BB expression pattern across different CD8⁺ T-cell fractions. The percentage of 4-1BB^{pos} cells was compared among the different T-cell fractions of total and NY-ESO-1₁₅₇₋₁₆₅-specific CD8⁺ T cells. Left panel shows representative flow cytometry plots. (D) 4-1BB expression according to differential PD-1 expression levels. The percentage of 4-1BB^{pos} cells was compared among PD-1^{high}, PD-1^{int} and PD-1^{neg} subpopulations of total and NY-ESO-1₁₅₇₋₁₆₅-specific CD8⁺ TILs. (E) Correlations between the percentage of 4-1BB^{pos} CD8⁺ TILs and PD-1^{high} CD8⁺ TILs among the total CD8⁺ TILs and NY-ESO-1₁₅₇-specific CD8⁺ TILs. Upper panel shows representative flow cytometry plots. Data are presented as mean ± SEM. **P* < 0.05; ***P* < 0.01; ****P* < 0.001. Abbreviation: ns, not significant.

we next investigated parameters of tumor reactivity (i.e., CD39 and CD103) and T-cell activation (i.e., CD38 and HLA-DR) among three distinct subpopulations of PD-1⁺ CD8⁺ TILs determined by differential 4-1BB and PD-1 expression levels: PD-1^{int}, 4-1BB^{neg}PD-1^{high}, and 4-1BB^{pos}PD-1^{high} subpopulations (Fig. 2A).

We first examined the proportion of a CD39⁺CD103⁺ CD8⁺ TIL subset representing tumor reactivity.⁽³¹⁾ The 4-1BB^{pos}PD-1^{high} subpopulation showed the highest percentages of CD39⁺CD103⁺ cells among both total and NY-ESO-1₁₅₇₋₁₆₅-specific CD8⁺ TILs, followed by the 4-1BB^{neg}PD-1^{high} and PD-1^{int} subpopulations (Fig. 2B). The percentage of activated T cells (CD38⁺HLA-DR⁺ cells) was higher among 4-1BB^{pos}PD-1^{high} CD8⁺ TILs than in 4-1BB^{neg}PD-1^{high} CD8⁺ TILs, with the lowest frequency among PD-1^{int} CD8⁺ TILs (Fig. 2C). Additionally, expression levels of the TCR-responsive transcription factors, interferon regulatory factor 4 (IRF4), basic leucine zipper transcription factor ATF-like (BATF) and nuclear factor of activated T cells c1 (NFATc1), were higher among 4-1BB^{pos}PD-1^{high} CD8⁺ TILs than among 4-1BB^{neg}PD-1^{high} and PD-1^{int} CD8⁺ TILs (Supporting Fig. S4).

To confirm the distinct activation-related features in 4-1BB-expressing CD8⁺ TILs, we performed RNA-seq of fluorescence-activated cell sorting (FACS)-sorted PD-1^{int}, 4-1BB^{neg}PD-1^{high}, and 4-1BB^{pos}PD-1^{high} CD8⁺ TILs. These subpopulations were compared with regard to the expression levels of four gene signatures that have been shown to represent T-cell activation⁽²³⁻²⁶⁾ (Fig. 2D). Notably, 4-1BB^{pos}PD-1^{high} CD8⁺ TILs showed substantial enrichment of all four T-cell activation gene

signatures compared to PD-1^{int} and 4-1BB^{neg}PD-1^{high} CD8⁺ TILs (Fig. 2E). Only two of four gene sets were enriched in the 4-1BB^{neg}PD-1^{high} subpopulation compared to the PD-1^{int} subpopulation (Fig. 2E).

Overall, these results suggest that 4-1BB^{pos}PD-1^{high} CD8⁺ TILs display immunophenotypes indicating higher degrees of T-cell activation and tumor reactivity, as well as distinct enrichment of genes related to T-cell activation. This highlights the heterogeneous activation status of exhausted CD8⁺ TILs according to 4-1BB expression.

PERCENTAGE OF 4-1BB^{pos} CD8⁺ TILs IS POSITIVELY CORRELATED WITH DEGREE OF CD8⁺ TIL ACTIVATION

To assess the implications of 4-1BB expression on CD8⁺ TILs on a per-patient basis, we examined the relationship between the percentage of 4-1BB^{pos} CD8⁺ TILs and activation-related features of CD8⁺ TILs. The percentage of 4-1BB^{pos} cells was positively correlated with the percentages of CD39⁺CD103⁺ cells and CD38⁺HLA-DR⁺ cells among total CD8⁺ TILs (Fig. 3A, upper panels), as well as among NY-ESO-1₁₅₇₋₁₆₅-specific CD8⁺ TILs (Fig. 3A, lower panels). On the other hand, the prominent correlations between the percentage of 4-1BB^{pos} CD8⁺ TILs and the percentages of CD39⁺CD103⁺ and CD38⁺HLA-DR⁺ cells in HCC were not universally observed across other cancer types (Supporting Fig. S5), possibly attributed to the lower percentages of 4-1BB^{pos} CD8⁺ TILs in other cancer types.

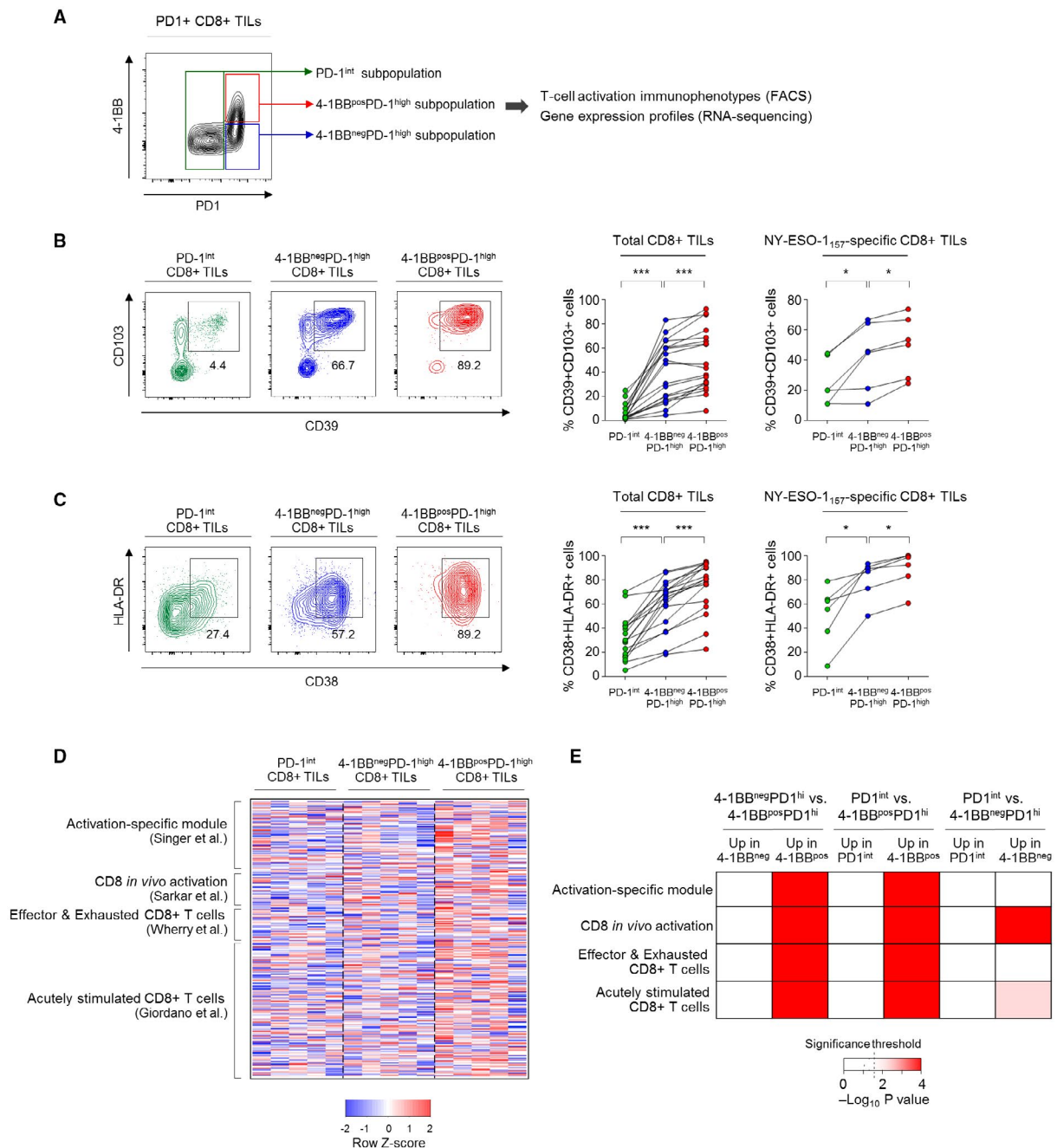


FIG. 2. 4-1BB-expressing PD-1^{high} CD8⁺ TILs feature immunophenotypically and transcriptionally prominent T-cell activation. (A) Representative flow cytometry plot showing subpopulations of PD-1⁺ CD8⁺ TILs according to differential expression of PD-1 and 4-1BB. (B,C) Percentages of CD39⁺CD103⁺ cells (B) and CD38⁺HLA-DR⁺ cells (C) among the PD-1^{int}, 4-1BB^{neg}PD-1^{high}, and 4-1BB^{pos}PD-1^{high} subpopulations of total and NY-ESO-1₁₅₇-specific CD8⁺ TILs. Left panels show representative flow cytometry plots (B,C). (D,E) RNA-seq data comparing expression of genes related to T-cell activation among FACS-sorted PD-1^{int}, 4-1BB^{neg}PD-1^{high} and 4-1BB^{pos}PD-1^{high} CD8⁺ TILs. (D) Heatmap showing expression levels of T-cell activation gene signatures among the PD-1^{int}, 4-1BB^{neg}PD-1^{high}, and 4-1BB^{pos}PD-1^{high} subpopulations. (E) Relative enrichment of T-cell activation gene signatures among PD-1^{int}, 4-1BB^{neg}PD-1^{high}, and 4-1BB^{pos}PD-1^{high} CD8⁺ TILs. Dashed line marks the significance threshold ($P = 0.05$). * $P < 0.05$; *** $P < 0.001$.

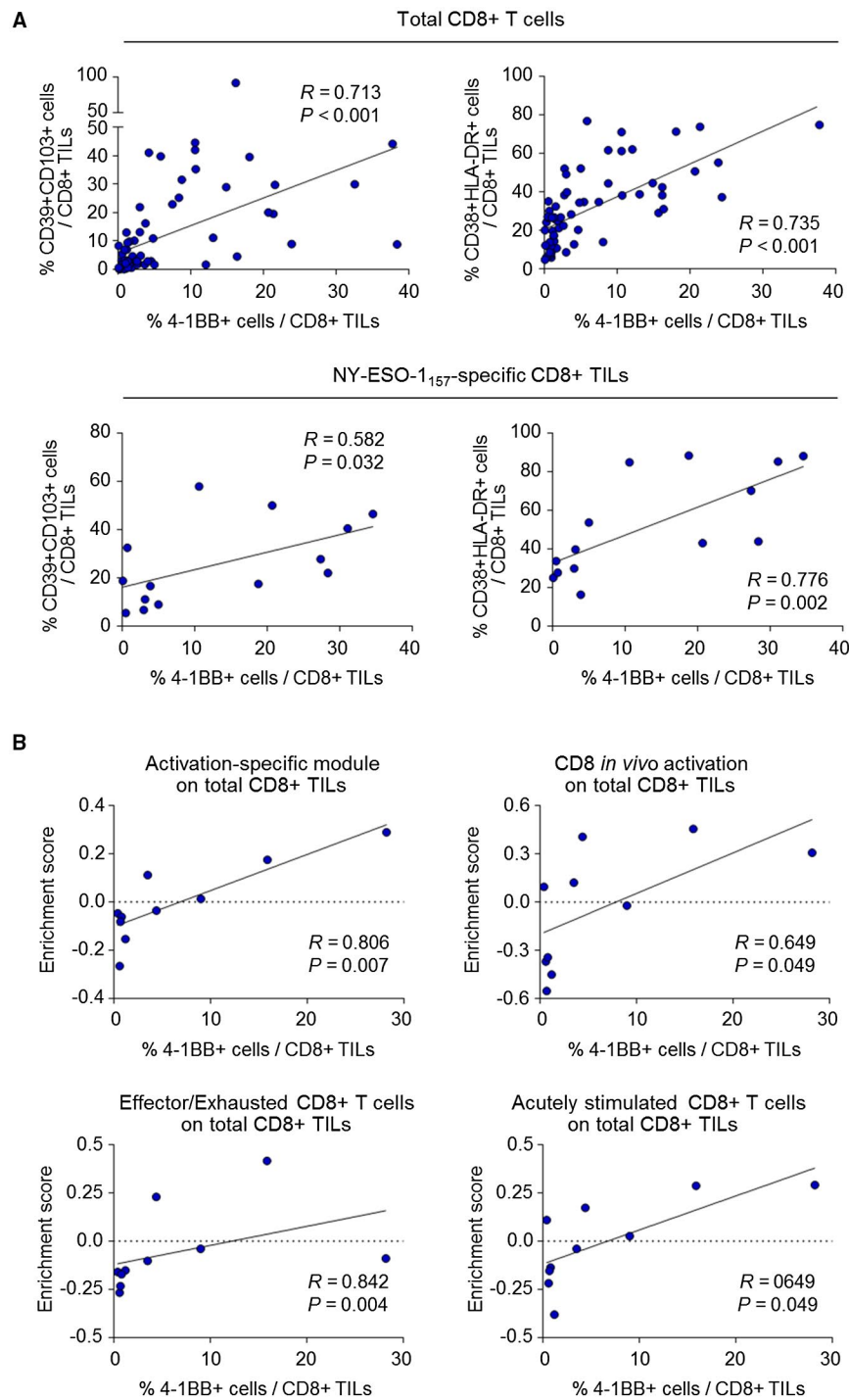


FIG. 3. The percentage of 4-1BB^{POS} CD8⁺ TILs is positively correlated with the degree of overall activation of CD8⁺ TILs. (A) Correlations between the percentage of 4-1BB^{POS} CD8⁺ TILs and the percentages of CD39⁺CD103⁺ cells and CD38⁺HLA-DR⁺ cells, among total CD8⁺ TILs (left panel) and NY-ESO-1₁₅₇₋₁₆₅-specific CD8⁺ TILs (right panel). (B) RNA-seq data from sorted total CD8⁺ TILs, analyzing the expression levels of T-cell activation gene signatures, represented as the enrichment score obtained by GSVA. Correlations between the percentage of 4-1BB^{POS} CD8⁺ TILs and enrichment scores of T-cell activation gene signatures were subsequently analyzed.

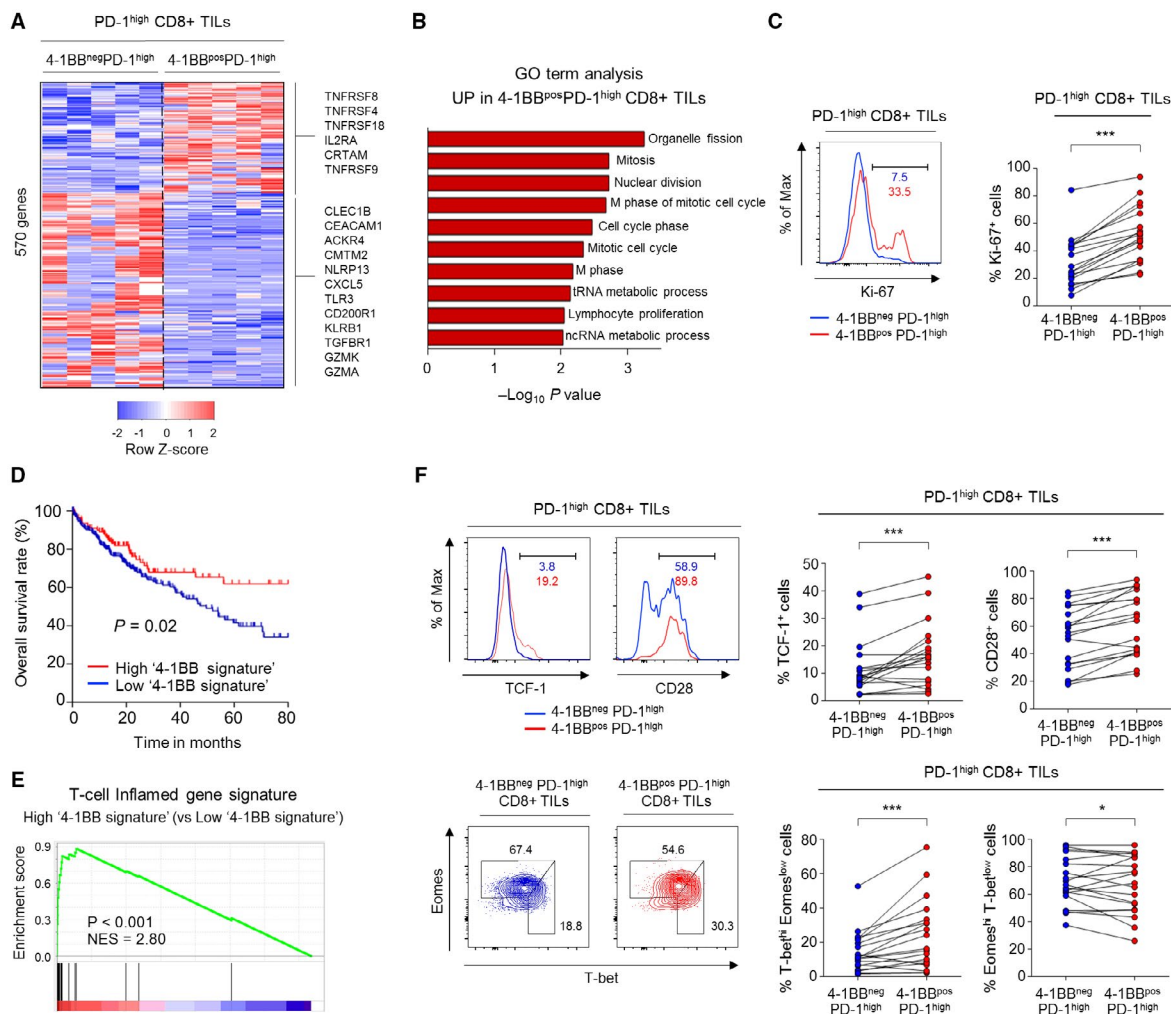


FIG. 4. 4-1BB^{pos}PD-1^{high} CD8⁺ TILs exhibited higher levels of markers indicating T-cell proliferation and reinvigoration compared to 4-1BB^{neg}PD-1^{high} CD8⁺ TILs. (A) Heatmap showing expression levels of 569 DEGs between 4-1BB^{neg}PD-1^{high} and 4-1BB^{pos}PD-1^{high} CD8⁺ TILs. (B) Gene Ontology analysis for the DEGs that were up-regulated in 4-1BB^{pos}PD-1^{high} CD8⁺ TILs compared to in 4-1BB^{neg}PD-1^{high} CD8⁺ TILs. (C) Percentage of Ki-67⁺ cells compared between 4-1BB^{pos}PD-1^{high} and 4-1BB^{neg}PD-1^{high} CD8⁺ TILs. Left panel shows representative flow cytometry plot. (D) Kaplan-Meier curve comparing survival outcomes among subgroups (i.e., high and low 4-1BB signature groups) of HCC patients in the TCGA cohort, according to expression of the 4-1BB signature. Cutoff was determined by the maximal chi-square method. (E) GSEA was performed to compare the enrichment of a T-cell-inflamed gene signature between the high and low 4-1BB signature groups. (F) Expression levels of parameters involved in T-cell reinvigoration (i.e., TCF-1, CD28, and T-bet/Eomes) were compared between 4-1BB^{pos}PD-1^{high} and 4-1BB^{neg}PD-1^{high} CD8⁺ TILs. Left panel shows representative flow cytometry plots. * $P < 0.05$; *** $P < 0.001$. Abbreviations: ACKR4, atypical chemokine receptor 4; CEACAM1, carcinoembryonic antigen-related cell adhesion molecule 1; CLEC1B, C-type lectin domain family 1 member B; CMTM2, CKLF-like MARVEL transmembrane domain-containing 2; CXCL5, C-X-C motif chemokine ligand 5; Eomes, eomesodermin; GO, Gene Ontology; GZMA, granzyme 1, cytotoxic T-lymphocyte-associated serine esterase 3; GZMK, granzyme K (serine protease, granzyme 3; tryptase II); IL2RA, interleukin-2 receptor agonist; KLRB1, killer cell lectin-like receptor B1; Max, maximum; ncRNA, noncoding RNA; NES, normalized enrichment score; NLRP13, NOD-like receptor family pyrin domain containing 13; T-bet, T-box-containing protein expressed in T cells; TGFB1, transforming growth factor beta receptor 1; tRNA, total RNA.

RNA-seq data from sorted total CD8⁺ TILs revealed that expression levels of T-cell activation gene signatures were positively correlated with the percentage of 4-1BB^{pos}

cells among CD8⁺ TILs (Fig. 3B). This suggests that the frequency of 4-1BB^{pos} CD8⁺ TILs indicate the degree of overall T-cell activation in the HCC microenvironment.

4-1BB^{pos}PD-1^{high} CD8⁺ TILs DISPLAY HIGHER LEVELS OF PARAMETERS INDICATING T-CELL PROLIFERATION AND REINVIGORATION THAN 4-1BB^{neg}PD-1^{high} CD8⁺ TILs

Next, we further investigated the immunological implications of 4-1BB expression specifically in highly exhausted CD8⁺ T cells in the HCC microenvironment. To this end, we directly compared 4-1BB^{pos} and 4-1BB^{neg} cells among PD-1^{high} CD8⁺ TILs with regard to differential gene expression and factors related to T-cell reinvigoration potential.

Examination of DEGs revealed that a total of 205 genes were up-regulated and 364 genes were down-regulated in 4-1BB^{pos}PD-1^{high} CD8⁺ TILs compared to 4-1BB^{neg}PD-1^{high} CD8⁺ TILs (Fig. 4A). The genes that were up-regulated in 4-1BB^{pos}PD-1^{high} CD8⁺ TILs compared to 4-1BB^{neg}PD-1^{high} CD8⁺ TILs included several genes encoding other costimulatory receptors (i.e., TNFRSF8, TNFRSF4, TNFRSF18, and class I MHC-restricted T-cell-associated molecule gene [CRTAM]; Fig. 4A). Gene ontology term analysis indicated enrichment of cell-cycle pathway genes among those that were up-regulated in 4-1BB^{pos}PD-1^{high} CD8⁺ TILs compared to 4-1BB^{neg}PD-1^{high} CD8⁺ TILs (Fig. 4B). This was further supported by the higher percentage of cells positive for the proliferation marker, Ki-67, within the 4-1BB^{pos}PD-1^{high} subpopulation compared to the 4-1BB^{neg}PD-1^{high} subpopulation, among both total and NY-ESO-1₁₅₇₋₁₆₅-specific CD8⁺ TILs (Fig. 4C and Supporting Fig. S6A). In contrast, genes related to cell-death pathways were down-regulated in 4-1BB^{pos}PD-1^{high} CD8⁺ TILs compared to 4-1BB^{neg}PD-1^{high} CD8⁺ TILs (Supporting Fig. S6B).

The top 50 genes that were significantly up- or down-regulated in 4-1BB^{pos}PD-1^{high} CD8⁺ TILs compared to 4-1BB^{neg}PD-1^{high} CD8⁺ TILs are summarized in Supporting Table S2. The top 50 genes up-regulated in 4-1BB^{pos}PD-1^{high} CD8⁺ TILs were defined as the “4-1BB signature.” Mean level of 4-1BB signature expression, as indicated by enrichment score, was highest in HCC compared to the other cancer types in the TCGA cohorts (Supporting Fig. S7A). We next examined the clinical implications of this 4-1BB signature using data from the TCGA HCC cohort and found that tumors with high 4-1BB signature were

associated with better survival outcomes compared to those with low 4-1BB signature (Fig. 4D). Moreover, compared to HCCs with low levels of 4-1BB signature, those with high levels of 4-1BB signature exhibited significant enrichment for a T-cell–inflamed gene module representing active IFN- γ response, cytotoxic effector function, and T-cell–activating cytokines that is reportedly associated with response to anti-PD-1 therapy^(32,33) (Fig. 4E). In an independent HCC cohort, we also identified superior survival outcomes and enrichment of the T-cell inflamed gene signature among the HCCs exhibiting high 4-1BB signature expression (Supporting Fig. S7B,C).

We further examined several parameters associated with T-cell reinvigoration potential by ICIs, including T-cell factor 1 (TCF-1),^(34,35) CD28,⁽³⁶⁾ and T-bet/Eomes.^(37,38) Compared to 4-1BB^{neg}PD-1^{high} CD8⁺ TILs, 4-1BB^{pos}PD-1^{high} CD8⁺ TILs had higher percentages of TCF-1⁺, CD28⁺, and T-bet^{high}/Eomes^{low} cells, which represent subpopulations potentially reinvigorated by ICIs (Fig. 4F and Supporting Fig. S8). On the other hand, the proportion of terminally differentiated Eomes^{high}/T-bet^{low} cells was lower in 4-1BB^{pos}PD-1^{high} CD8⁺ TILs compared to 4-1BB^{neg}PD-1^{high} CD8⁺ TILs (Fig. 4F and Supporting Fig. S8).

Collectively, our results indicate that the 4-1BB-related gene expression profile was associated with active antitumor response and that the subpopulation of 4-1BB-expressing CD8⁺ TILs may retain higher proliferative and reinvigoration potential among highly exhausted CD8⁺ TILs.

4-1BB COSTIMULATION FURTHER ENHANCES FUNCTION OF CD8⁺ TILs AND ANTI-PD-1-MEDIATED CD8⁺ TIL REINVIGORATION

Finally, we investigated whether 4-1BB costimulation with agonistic antibodies against 4-1BB could enhance the function of CD8⁺ TILs. *In vitro* functional assays revealed that 4-1BB costimulation significantly enhanced CD8⁺ TIL proliferation, as indicated by SI (Fig. 5A) as well as IFN- γ and TNF- α production by CD8⁺ TILs (Supporting Fig. S9). To further characterize CD8⁺ TILs that favorably responded to anti-4-1BB treatment, we subdivided CD8⁺ TIL samples into two subgroups based on their degree of functional response to anti-4-1BB

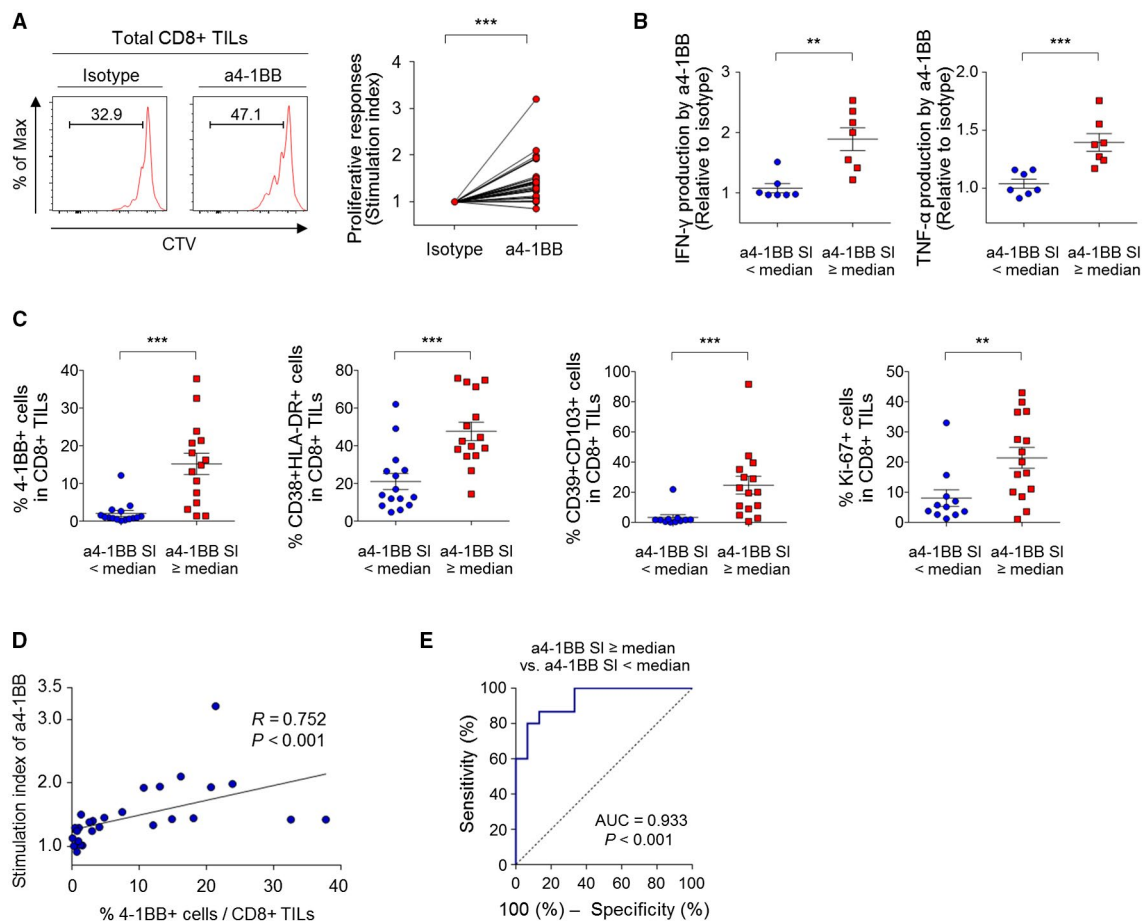


FIG. 5. 4-1BB costimulation enhances the function of CD8⁺ TILs, especially in HCCs exhibiting prominent T-cell activation. (A) Investigation of the effect of 4-1BB costimulation on the proliferative response of CD8⁺ TILs, as indicated by SI. (B,C,E) Study patients were subdivided into two subgroups using the median SI by anti-4-1BB as the cutoff (\geq the median SI vs. $<$ the median SI). (B) Comparison between the two subgroups of the relative increases of IFN- γ and TNF- α production by CD8⁺ TILs with 4-1BB costimulation. (C) Comparison between the two subgroups of the percentages of 4-1BB⁺, CD39⁺CD103⁺, CD38⁺HLA-DR⁺, and Ki-67⁺ cells among CD8⁺ TILs. (D) Correlation between the percentage of 4-1BB^{pos} CD8⁺ TILs and the SI by 4-1BB costimulation. (E) Receiver operating characteristic curve estimating the performance of the percentages of 4-1BB^{pos} CD8⁺ TILs with regard to distinguishing the two subgroups. Data are presented as mean \pm SEM. (B,C) ** $P < 0.01$; *** $P < 0.001$. Abbreviation: Max, maximum.

treatment, using median SI value as the cutoff (\geq the median SI vs. $<$ the median SI). In accord with the proliferation assay results, compared to CD8⁺ TILs with lower SI values, CD8⁺ TILs with higher SI values exhibited greater relative increases of IFN- γ and TNF- α production by CD8⁺ TILs with anti-4-1BB treatment (Fig. 5B). More important, compared to those with lower SI values, CD8⁺ TILs with higher SI values exhibited significantly larger percentages of 4-1BB⁺, CD39⁺CD103⁺, CD38⁺HLA-DR⁺, and Ki-67⁺ cells (Fig. 5C). We also identified a robust correlation between functional anti-4-1BB responses and percentage of 4-1BB^{pos} CD8⁺ TILs (Fig. 5D). Area

under the curve analysis revealed that the percentage of 4-1BB^{pos} CD8⁺ TILs reliably distinguished the subgroup with a higher SI value by anti-4-1BB treatment (i.e., \geq median SI; Fig. 5E).

Recent clinical trials of anti-PD-1 therapy in HCC patients suggest a need to improve its therapeutic efficacy.^(2,3) Thus, we next examined whether 4-1BB costimulation could further enhance anti-PD-1-mediated T-cell reinvigoration. While single PD-1 blockade restored the abilities of CD8⁺ TILs to proliferate and produce IFN- γ and TNF- α , the combination of 4-1BB costimulation and PD-1 blockade further enhanced the abilities of CD8⁺ TILs to

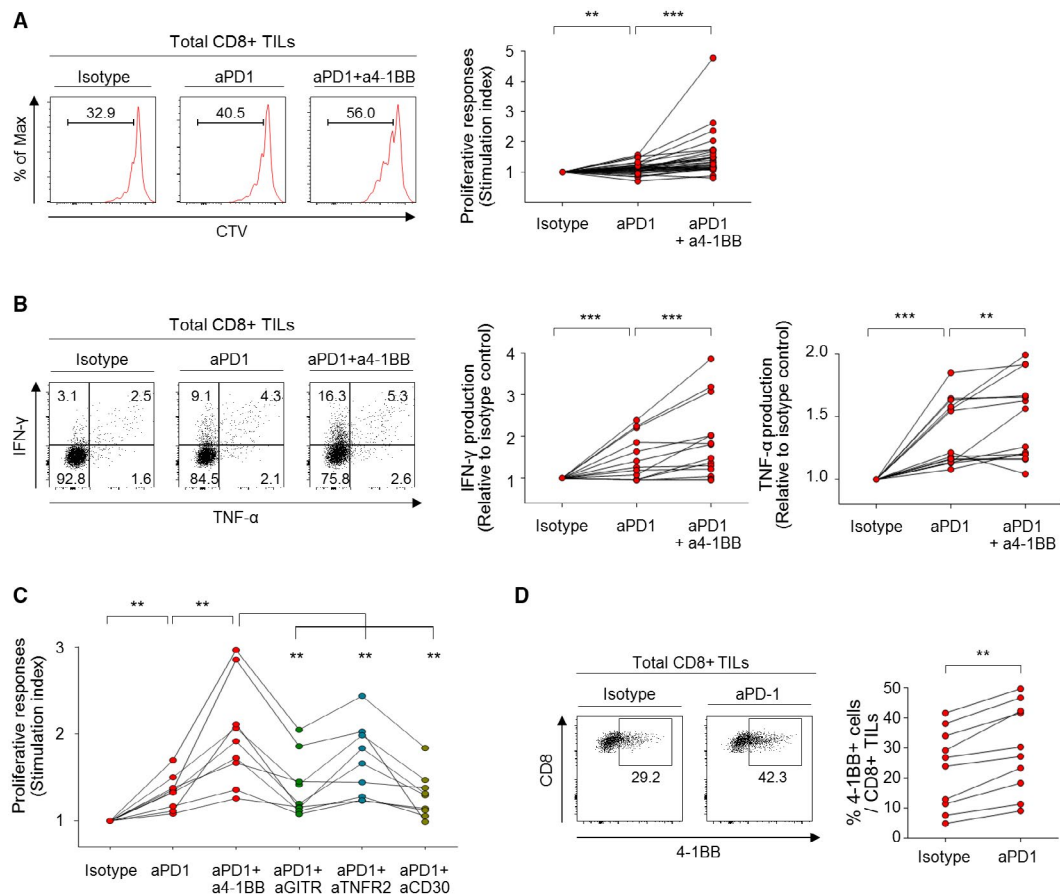


FIG. 6. 4-1BB costimulation further enhances anti-PD-1-mediated CD8⁺ TIL reinvigoration. (A,B) Efficacy of the combination of 4-1BB costimulation and PD-1 blockade compared to the efficacy of PD-1 blockade or isotype control in terms of proliferative response (A) and cytokine production (B). (C) Comparison of the proliferative functional response of CD8⁺ TILs with various combinations of PD-1 blockade and costimulatory agonists (i.e., anti-4-1BB, anti-GITR, anti-TNFR2, and anti-CD30). (D) The percentage of 4-1BB^{pos} cells was compared between samples treated with PD-1 blocking antibodies versus isotype control upon anti-CD3 stimulation (10 ng/mL) for 48 hours. In (A) and (C), data are presented as the SI of CD8⁺ TILs. In (B), data are presented as the relative ratio of the percentage of CD8⁺ TILs that produce IFN- γ and TNF- α by combined 4-1BB costimulation and PD-1 blockade or PD-1 blockade alone, compared to that by isotype control. ** $P < 0.01$; *** $P < 0.001$. Abbreviation: Max, maximum.

proliferate (Fig. 6A) and produce IFN- γ and TNF- α (Fig. 6B). Again, the percentage of 4-1BB^{pos} CD8⁺ TILs was positively correlated with the SI of combined 4-1BB costimulation and PD-1 blockade (Supporting Fig. S10A) and predicted the patient subgroup that exhibited more-pronounced functional CD8⁺ TIL responses to this combined treatment (i.e., \geq median SI by anti-4-1BB plus anti-PD-1; Supporting Fig. S10B).

We then compared the efficacies of various combinations of PD-1 blockade and costimulatory agonists, revealing that the combination of anti-4-1BB plus anti-PD-1 led to more pronounced functional

CD8⁺ TIL responses compared to other combinations (i.e., anti-PD-1 plus anti-GITR, anti-TNFR2, or anti-CD30; Fig. 6C). PD-1 blockade-mediated T-cell reinvigoration was accompanied by up-regulation of 4-1BB on CD8⁺ TILs (Fig. 6D), indicating that PD-1 blockade may have beneficial effects on CD8⁺ TILs as part of immunotherapies targeting 4-1BB.

Discussion

The therapeutic potential of targeting costimulatory receptors is currently under early clinical evaluation;

however, much remains unknown about the biological and clinical implications of these receptors, which are essential for the rational design of immunotherapies. In this study, we investigated costimulatory receptor expression patterns on CD8⁺ TILs as well as the heterogeneity of T-cell activation among exhausted CD8⁺ TILs in HCC. Compared to other examined activation-induced costimulatory receptors, we found that 4-1BB was most prominently expressed on CD8⁺ TILs, with expression almost exclusively on highly exhausted PD-1^{high} CD8⁺ TILs. 4-1BB^{pos}PD-1^{high} CD8⁺ TILs displayed immunophenotypic and transcriptomic features of prominent T-cell activation and higher levels of tumor reactivity markers. Among PD-1^{high} CD8⁺ TILs, 4-1BB-expressing cells exhibited higher levels of proliferation and reinvigoration of potential markers. Finally, we showed that 4-1BB costimulation with agonistic antibodies enhanced CD8⁺ TIL function and further enhanced anti-PD-1-mediated CD8⁺ TIL reinvigoration, especially in HCCs exhibiting prominent T-cell activation.

This was a study to comprehensively characterize costimulatory receptor expression on CD8⁺ TILs and the associated T-cell activation features in HCC patients. Previous studies describe the expression of 4-1BB and other costimulatory receptors on CD8⁺ T cells, but earlier investigations have been limited in that they either used CD8⁺ T cells from peripheral blood⁽³⁹⁾ or simply confirmed costimulatory receptor expression on tumor-infiltrating T cells in HCC.^(19,20) In HCC, 4-1BB expression was most prominent among the tested activation-induced costimulatory receptors in CD8⁺ TILs. However, this was not the case for the other examined cancer types. Additionally, compared to the other cancer types tested, HCC had a higher percentage of 4-1BB^{pos} CD8⁺ TILs, but had similar or even lower percentages of CD8⁺ TILs expressing other costimulatory receptors. Thus, the substantial differences in these features among various cancer types necessitate the detailed delineation of 4-1BB-related T-cell activation in HCC. Together with high levels of the 4-1BB-related gene signature in HCC, these highlight the prominent 4-1BB expression on CD8⁺ TILs and distinct 4-1BB-related features as notable aspects of HCC that are not universally observed in other cancer types.

Another interesting finding is that 4-1BB was almost exclusively expressed on PD-1^{high} CD8⁺ TILs, which reportedly represent highly exhausted

and tumor-reactive CD8⁺ TILs.^(18,30) We recently demonstrated that PD-1^{high} CD8⁺ TILs exhibit features of more progressed T-cell exhaustion compared to PD-1^{int} and PD-1^{neg} CD8⁺ TILs and that HCCs with higher proportions of PD-1^{high} CD8⁺ TILs are enriched for the T-cell-inflamed gene signature.⁽¹⁸⁾ Similarly, Thommen et al. examined patients with non-small-cell lung cancer displaying typical phenotypic features of T-cell exhaustion and reported that PD-1^{high} CD8⁺ TILs were associated with higher tumor recognition capacity and response to anti-PD-1 therapy.⁽³⁰⁾ These findings suggest that PD-1^{high} CD8⁺ TILs indicate active engagement against tumors and resultant exhausted phenotypes. Thus, expression of 4-1BB on PD-1^{high} CD8⁺ TILs suggests that 4-1BB may deliver costimulatory signals specifically to highly exhausted CD8⁺ TILs that have rigorously engaged in antitumor responses.

T-cell exhaustion arises because of excessive and prolonged T-cell activation to prevent immunopathology; therefore, these two states are closely interconnected and share features related to the cell-cycle pathway, T-cell migration, and cytotoxic effector function.^(23,25,26,40,41) Indeed, recent single-cell transcriptomic analyses indicate that a proportion of CD8⁺ TILs that were previously identified as exhausted are indeed highly proliferating and undergoing a dynamic differentiation process.^(42,43) This highlights the importance of distinguishing the subset of exhausted T cells in a viable T-cell activation state. Compared to PD-1^{int} and 4-1BB^{neg}PD-1^{high} CD8⁺ TILs, we found that 4-1BB^{pos}PD-1^{high} CD8⁺ TILs showed the highest levels of T-cell activation markers and TCR-responsive transcription factors as well as significant enrichment for T-cell-activation-related gene signatures. Importantly, a T-cell activation gene signature that is uncoupled from dysfunction⁽²³⁾ was specifically enriched in the 4-1BB^{pos}PD-1^{high} subpopulation, but not in the 4-1BB^{neg}PD-1^{high} and PD-1^{int} subpopulations. 4-1BB^{pos}PD-1^{high} CD8⁺ TILs also displayed the highest proportion of the tumor-reactive CD39⁺CD103⁺ subset, indicating that the prominent T-cell activation likely resulted from increased tumor reactivity of 4-1BB^{pos} cells. On the other hand, the percentage of 4-1BB^{pos} CD8⁺ TILs was positively correlated with the parameters of T-cell activation analyzed on an individual basis, indicating that 4-1BB may be a useful indicator of the overall activation status of exhausted CD8⁺ TILs.

Direct comparison between 4-1BB^{pos} and 4-1BB^{neg} cells among highly exhausted PD-1^{high} CD8⁺ TILs revealed substantial differences in the gene expression profiles and in parameters of T-cell proliferation and reinvigoration. Indeed, genes up-regulated in 4-1BB^{pos}PD-1^{high} CD8⁺ TILs were associated with the cell-cycle pathway and these cells displayed higher percentages of proliferation markers. Additionally, among PD-1^{high} CD8⁺ TILs, 4-1BB^{pos} cells retained a higher proportion of cells involved in T-cell reinvigoration than 4-1BB^{neg} cells. Whereas 4-1BB expression was previously shown to represent the tumor reactivity of CD8⁺ TILs,⁽⁴⁴⁾ our study highlights immunological implications of 4-1BB expression in exhausted CD8⁺ TILs: (1) The T-cell-activating receptor, 4-1BB, is almost exclusively expressed on highly exhausted PD-1^{high} CD8⁺ TILs; (2) 4-1BB^{pos} CD8⁺ TILs harbor the highest degree of T-cell activation, as well as proliferative and reinvigoration potential among highly exhausted CD8⁺ TILs; and (3) 4-1BB expression represents the overall activation status of CD8⁺ TILs. Together, our findings indicate that 4-1BB expression identifies a highly activated and immunologically viable population of phenotypically exhausted CD8⁺ TILs in HCC.

Another strength of our study is the identification of a T-cell activation gene set that could help find targets to maximize T-cell activation signals in HCC microenvironments. The 4-1BB gene signature, derived from differential 4-1BB expression among PD-1^{high} CD8⁺ TILs, was validated as predicting survival outcomes of patients in the TCGA cohort and in an independent HCC cohort. This suggests that the higher degree of T-cell activation associated with 4-1BB expression may reflect a robust antitumor response that leads to improved survival outcomes in HCC patients. Furthermore, HCCs with higher 4-1BB signature expression showed enrichment of the T-cell-inflamed gene signature, suggesting that 4-1BB-related T-cell activation directs active IFN- γ and cytotoxic antitumor T-cell responses, which are also associated with anti-PD-1 response.^(32,33) This gene set will be an important resource for mining additional key genes and pathways involved in T-cell activation against HCC. It will also be interesting to validate whether this gene signature may be useful as a predictive biomarker for ICIs.

Using the *in vitro* functional assay system, we provide a demonstration that 4-1BB costimulation promoted the functional enhancement of CD8⁺

TILs from HCC patients. Importantly, CD8⁺ TILs exhibiting higher degrees of T-cell activation, tumor reactivity, and proliferation were associated with a better functional response to anti-4-1BB treatment compared to those with low levels of pre-existing T-cell activation. These findings suggest that anti-4-1BB therapy may be more effective in HCC patients exhibiting prominent T-cell activation, which is linked to higher 4-1BB expression on CD8⁺ TILs. Moreover, 4-1BB expression reliably distinguished cases with a favorable CD8⁺ TIL response to anti-4-1BB treatment. Therefore, 4-1BB expression on CD8⁺ TILs may be useful for guiding the selection of patients who are likely to favorably respond to anti-4-1BB treatment. These insights support the potential development of a clinical-grade biomarker based on 4-1BB expression such as immunohistochemical staining of 4-1BB for HCC patients receiving anti-4-1BB therapy.

We also found that 4-1BB costimulation could further enhance PD-1 blockade-mediated T-cell reinvigoration. The objective response rates of anti-PD-1 therapy are reportedly around 20% in HCC patients^(2,3); thus, there is an urgent need to improve the therapeutic efficacy of immunotherapy involving anti-PD-1 therapy. Our findings indicate that 4-1BB costimulation may be a potent therapeutic option in conjunction with anti-PD-1 therapy. Our finding that PD-1 blockade-mediated T-cell reinvigoration was accompanied by increased 4-1BB expression implies that the combination of 4-1BB costimulation and PD-1 blockade can act synergistically. Together, our results provide insights that may guide the design of immunotherapy involving 4-1BB costimulation. Although an issue has been raised regarding the hepatotoxicity of the 4-1BB agonist, urelumab, it is generally considered that this problem can be overcome with urelumab dose adjustment,⁽⁴⁵⁾ use of the other 4-1BB agonist, utolimumab,⁽⁴⁶⁾ and with agents having tumor-specific properties^(5,11,47,48) or that exhibit balanced agonistic strength with Fc gamma receptor (Fc γ R) affinity.^(14,49) Future research may be required to further study the effects of 4-1BB costimulation on other immune subsets, such as regulatory T cells,⁽¹⁴⁾ and the interactions with Fc γ Rs of the antibodies^(14,49) to support the optimal application of anti-4-1BB therapy.

In conclusion, we demonstrated a distinct 4-1BB-associated T-cell activation state among exhausted CD8⁺ TILs in HCC. Our results provide rationale

and evidence for the logical design of immunotherapies targeting costimulatory receptor 4-1BB, as well as delineate immunological and clinical implications of T-cell activation status in the HCC microenvironment. Treatment strategies involving 4-1BB costimulation may be a promising therapeutic option for enhancing T-cell activation against HCC. Future clinical studies are warranted to evaluate the efficacy of 4-1BB agonists in HCC patients.

Author Contributions: H.D.K. and S.H.P. contributed to the conceptual design of the study and writing the manuscript. H.D.K., S.P., S.J., Y.J.L., H.L., S.M.H., J.Y.L., S.K., H.K.K., B.S.M., J.H.C., G.W.S., Y.S.J., E.C.S., S.H., and S.H.P. were involved in data acquisition. H.D.K., S.P., S.J., Y.S.J., E.C.S., and S.H.P. were involved in data analysis and interpretation.

REFERENCES

- Wei SC, Duffy CR, Allison JP. Fundamental mechanisms of immune checkpoint blockade therapy. *Cancer Discov* 2018;8:1069-1086.
- El-Khoueiry AB, Sangro B, Yau T, Crocenzi TS, Kudo M, Hsu C, et al. Nivolumab in patients with advanced hepatocellular carcinoma (CheckMate 040): an open-label, non-comparative, phase 1/2 dose escalation and expansion trial. *Lancet* 2017;389:2492-2502.
- Zhu AX, Finn RS, Edeline J, Cattan S, Ogasawara S, Palmer D, et al. Pembrolizumab in patients with advanced hepatocellular carcinoma previously treated with sorafenib (KEYNOTE-224): a non-randomised, open-label phase 2 trial. *Lancet Oncol* 2018;19:940-952.
- Greten TF, Lai CW, Li G, Staveley-O'Carroll KF. Targeted and immune-based therapies for hepatocellular carcinoma. *Gastroenterology* 2019;156:510-524.
- Mayes PA, Hance KW, Hoos A. The promise and challenges of immune agonist antibody development in cancer. *Nat Rev Drug Discov* 2018;17:509-527.
- Schaer DA, Hirschhorn-Cymerman D, Wolchok JD. Targeting tumor-necrosis factor receptor pathways for tumor immunotherapy. *J Immunother Cancer* 2014;2:7.
- Sanmamed MF, Pastor F, Rodriguez A, Perez-Gracia JL, Rodriguez-Ruiz ME, Jure-Kunkel M, et al. Agonists of co-stimulation in cancer immunotherapy directed against CD137, OX40, GITR, CD27, CD28, and ICOS. *Semin Oncol* 2015;42:640-655.
- Chen L, Flies DB. Molecular mechanisms of T cell co-stimulation and co-inhibition. *Nat Rev Immunol* 2013;13:227-242.
- Ward-Kavanagh LK, Lin WW, Sedy JR, Ware CF. The TNF receptor superfamily in co-stimulating and co-inhibitory responses. *Immunity* 2016;44:1005-1019.
- Long AH, Haso WM, Shern JF, Wanhainen KM, Murgai M, Ingaramo M, et al. 4-1BB costimulation ameliorates T cell exhaustion induced by tonic signaling of chimeric antigen receptors. *Nat Med* 2015;21:581-590.
- Chester C, Sanmamed MF, Wang J, Melero I. Immunotherapy targeting 4-1BB: mechanistic rationale, clinical results, and future strategies. *Blood* 2018;131:49-57.
- Vezys V, Penalzo-MacMaster P, Barber DL, Ha SJ, Konieczny B, Freeman GJ, et al. 4-1BB signaling synergizes with programmed death ligand 1 blockade to augment CD8 T cell responses during chronic viral infection. *J Immunol* 2011;187:1634-1642.
- Melero I, Shuford WW, Newby SA, Aruffo A, Ledbetter JA, Hellström KE, et al. Monoclonal antibodies against the 4-1BB T-cell activation molecule eradicate established tumors. *Nat Med* 1997;3:682-685.
- Buchan SL, Dou L, Remer M, Booth SG, Dunn SN, Lai C, et al. Antibodies to costimulatory receptor 4-1BB enhance anti-tumor immunity via T regulatory cell depletion and promotion of CD8 T cell effector function. *Immunity* 2018;49:958-970.e7.
- Tumeh PC, Harview CL, Yearley JH, Shintaku IP, Taylor EJ, Robert L, et al. PD-1 blockade induces responses by inhibiting adaptive immune resistance. *Nature* 2014;515:568-571.
- Huang AC, Postow MA, Orlowski RJ, Mick R, Bengsch B, Manne S, et al. T-cell invigoration to tumour burden ratio associated with anti-PD-1 response. *Nature* 2017;545:60-65.
- Daud AI, Loo K, Pauli ML, Sanchez-Rodriguez R, Sandoval PM, Taravati K, et al. Tumor immune profiling predicts response to anti-PD-1 therapy in human melanoma. *J Clin Invest* 2016;126:3447-3452.
- Kim HD, Song GW, Park S, Jung MK, Kim MH, Kang HJ, et al. Association between expression level of PD1 by tumor-infiltrating CD8(+) T cells and features of hepatocellular carcinoma. *Gastroenterology* 2018;155:1936-1950.e17.
- Lim CJ, Lee YH, Pan L, Lai L, Chua C, Wasser M, et al. Multidimensional analyses reveal distinct immune microenvironment in hepatitis B virus-related hepatocellular carcinoma. *Gut* 2019;68:916-927.
- Chew V, Lai L, Pan L, Lim CJ, Li J, Ong R, et al. Delineation of an immunosuppressive gradient in hepatocellular carcinoma using high-dimensional proteomic and transcriptomic analyses. *Proc Natl Acad Sci U S A* 2017;114:E5900-E5909.
- Love M, Anders S, Huber W. Differential analysis of count data—the DESeq2 package. *Genome Biol* 2014;15(10):1186.
- Subramanian A, Tamayo P, Mootha VK, Mukherjee S, Ebert BL, Gillette MA, et al. Gene set enrichment analysis: a knowledge-based approach for interpreting genome-wide expression profiles. *Proc Natl Acad Sci U S A* 2005;102:15545-15550.
- Singer M, Wang C, Cong L, Marjanovic ND, Kowalczyk MS, Zhang H, et al. A distinct gene module for dysfunction uncoupled from activation in tumor-infiltrating T cells. *Cell* 2016;166:1500-1511.e9.
- Sarkar S, Kalia V, Haining WN, Konieczny BT, Subramanian S, Ahmed R. Functional and genomic profiling of effector CD8 T cell subsets with distinct memory fates. *J Exp Med* 2008;205:625-640.
- Wherry EJ, Ha SJ, Kaech SM, Haining WN, Sarkar S, Kalia V, et al. Molecular signature of CD8+ T cell exhaustion during chronic viral infection. *Immunity* 2007;27:670-684.
- Giordano M, Henin C, Maurizio J, Imbratta C, Bourdely P, Buferne M, et al. Molecular profiling of CD8 T cells in autochthonous melanoma identifies Maf as driver of exhaustion. *EMBO J* 2015;34:2042-2058.
- Hanzelmann S, Castelo R, Guinney J. GSEA: gene set variation analysis for microarray and RNA-seq data. *BMC Bioinformatics* 2013;14:7.
- Grinchuk OV, Yenamandra SP, Iyer R, Singh M, Lee HK, Lim KH, et al. Tumor-adjacent tissue co-expression profile analysis reveals pro-oncogenic ribosomal gene signature for prognosis of resectable hepatocellular carcinoma. *Mol Oncol* 2018;12:89-113.
- Miller R, Siegmund D. Maximally selected chi square statistics. *Biometrics* 1982;38:1011-1016.
- Thommen DS, Koelzer VH, Herzig P, Roller A, Trefny M, Dimeloe S, et al. A transcriptionally and functionally distinct PD-1(+) CD8(+) T cell pool with predictive potential in non-small-cell lung cancer treated with PD-1 blockade. *Nat Med* 2018;24:994-1004.

- 31) **Duhen T, Duhen R**, Montler R, Moses J, Moudgil T, de Miranda NF, et al. Co-expression of CD39 and CD103 identifies tumor-reactive CD8 T cells in human solid tumors. *Nat Commun* 2018;9:2724.
- 32) Ayers M, Luceford J, Nebozhyn M, Murphy E, Loboda A, Kaufman DR, et al. IFN-gamma-related mRNA profile predicts clinical response to PD-1 blockade. *J Clin Invest* 2017;127:2930-2940.
- 33) Cristescu R, Mogg R, Ayers M, Albright A, Murphy E, Yearley J, et al. Pan-tumor genomic biomarkers for PD-1 checkpoint blockade-based immunotherapy. *Science* 2018;362:eaar3593.
- 34) Siddiqui I, Schauble K, Chennupati V, Fuertes Marraco SA, Calderon-Copete S, Pais Ferreira D, et al. Intratumoral Tcf1(+) PD-1(+)/CD8(+) T cells with stem-like properties promote tumor control in response to vaccination and checkpoint blockade immunotherapy. *Immunity* 2019;50:195-211.e10.
- 35) **Utzhneider DT, Charmoy M, Chennupati V**, Pousse L, Ferreira DP, Calderon-Copete S, et al. T cell factor 1-expressing memory-like CD8(+) T cells sustain the immune response to chronic viral infections. *Immunity* 2016;45:415-427.
- 36) Kamphorst AO, Wieland A, Nasti T, Yang S, Zhang R, Barber DL, et al. Rescue of exhausted CD8 T cells by PD-1-targeted therapies is CD28-dependent. *Science* 2017;355:1423-1427.
- 37) Blackburn SD, Shin H, Freeman GJ, Wherry EJ. Selective expansion of a subset of exhausted CD8 T cells by alphaPD-L1 blockade. *Proc Natl Acad Sci U S A* 2008;105:15016-15021.
- 38) Paley MA, Kroy DC, Odorizzi PM, Johnnidis JB, Dolfi DV, Barnett BE, et al. Progenitor and terminal subsets of CD8+ T cells cooperate to contain chronic viral infection. *Science* 2012;338:1220-1225.
- 39) Inada Y, Mizukoshi E, Seike T, Tamai T, Iida N, Kitahara M, et al. Characteristics of immune response to tumor-associated antigens and immune cell profile in patients with hepatocellular carcinoma. *HEPATOLOGY* 2019;69:653-665.
- 40) Fuertes Marraco SA, Neubert NJ, Verdeil G, Speiser DE. Inhibitory receptors beyond T cell exhaustion. *Front Immunol* 2015;6:310.
- 41) **Tirosh I, Izar B**, Prakadan SM, Wadsworth MH, Treacy D, Trombetta JJ, et al. Dissecting the multicellular ecosystem of metastatic melanoma by single-cell RNA-seq. *Science* 2016;352:189-196.
- 42) **Li H, van der Leun AM, Yofe I**, Lubling Y, Gelbard-Solodkin D, van Akkooi ACJ, et al. Dysfunctional CD8 T cells form a proliferative, dynamically regulated compartment within human melanoma. *Cell* 2019;176:775-789.e18.
- 43) **Zhang L, Yu X, Zheng L**, Zhang Y, Li Y, Fang Q, et al. Lineage tracking reveals dynamic relationships of T cells in colorectal cancer. *Nature* 2018;564:268-272.
- 44) Ye Q, Song DG, Poussin M, Yamamoto T, Best A, Li C, et al. CD137 accurately identifies and enriches for naturally occurring tumor-reactive T cells in tumor. *Clin Cancer Res* 2014;20:44-55.
- 45) **Segal NH, Logan TF**, Hodi FS, McDermott D, Melero I, Hamid O, et al. Results from an integrated safety analysis of urelumab, an agonist anti-CD137 monoclonal antibody. *Clin Cancer Res* 2017;23:1929-1936.
- 46) Segal NH, He AR, Doi T, Levy R, Bhatia S, Pishvaian MJ, et al. Phase I study of single-agent utomilumab (PF-05082566), a 4-1BB/CD137 agonist, in patients with advanced cancer. *Clin Cancer Res* 2018;24:1816-1823.
- 47) Compte M, Harwood SL, Munoz IG, Navarro R, Zonca M, Perez-Chacon G, et al. A tumor-targeted trimeric 4-1BB-agonistic antibody induces potent anti-tumor immunity without systemic toxicity. *Nat Commun* 2018;9:4809.
- 48) **Claus C, Ferrara C, Xu W**, Sam J, Lang S, Uhlenbrock F, et al. Tumor-targeted 4-1BB agonists for combination with T cell bispecific antibodies as off-the-shelf therapy. *Sci Transl Med* 2019;11:eaav5989.
- 49) **Qi X, Li F**, Wu Y, Cheng C, Han P, Wang J, et al. Optimization of 4-1BB antibody for cancer immunotherapy by balancing agonistic strength with FcγR2b affinity. *Nat Commun* 2019;10:2141.

Author names in bold designate shared co-first authorship.

Supporting Information

Additional Supporting Information may be found at onlinelibrary.wiley.com/doi/10.1002/hep.30881/supinfo.